

A Theoretical Study of NH_4^- and PH_4^-

Nikita Matsunaga and Mark S. Gordon*

Department of Chemistry, Iowa State University, Ames, Iowa 50011-3111

Received: April 18, 1995; In Final Form: June 2, 1995[⊗]

The potential energy surfaces of NH_4^- and PH_4^- were investigated using *ab initio* electronic structure calculations. Additivity of correlation and basis set effects was used to estimate relative energies. The tetrahedral structures of NH_4^- and PH_4^- are predicted to be minima on the respective potential energy surfaces. *Ab initio* classical trajectory calculations were carried out in order to elucidate possible dissociation paths of tetrahedral ions. The dissociation barrier was estimated to be 32.5 kcal/mol for NH_4^- and 5.5 kcal/mol for PH_4^- . Ionization potentials for the tetrahedral structures of NH_4^- and PH_4^- were calculated to be 0.39 and 0.32 eV, respectively.

Introduction

Structures in which a central atom is surrounded by more than the usual octet of electrons are sometimes referred to as hypervalency, and there are many synthetic examples of hypervalent compounds in the literature.¹ Such species are most common when the central atom is in the third period or lower periods, such as five-coordinate silicon species.^{1b,c} Several studies of hypervalent silicon and aluminum have been performed in this laboratory.²

There have been a number of explanations for how the expanded octet is achieved to obtain hypervalency. One of the oldest explanations, due to Pauling,³ describes hypervalency in pentacoordinated species by invoking d orbitals to construct sp^3d hybrid orbitals. However, the existence and the structures of these compounds are readily explained by molecular orbital theory without d-orbital participation. For an excellent discussion of this topic, the reader is referred to the paper by Reed and Schleyer.⁴ This issue was placed in an interesting perspective by Cooper *et al.*,⁵ who suggest that it is the democratic right of every valence electron to take part in chemical bonding if it so desires. In other words, valence electrons can participate in bonding if there is sufficient energy incentive.

The hypervalent NH_4^- anion has been observed via Fourier-transform mass spectrometry⁶ using a deuterium labeling study. The authors have concluded that the observed ion is best described as a hydride ion solvated by an ammonia molecule. Other experimental evidence, from photoelectron spectroscopy,⁷ suggests that tetrahedral NH_4^- exists on the potential energy surfaces (PESs).

Several theoretical calculations have been done to date.^{8–16} The complex between NH_3 and H^- , in which the hydride ion is almost collinear with one of the N–H bonds, has been speculated to be a global minimum on the potential energy surface. Also, the tetrahedral structure was predicted^{8,14–16} to be a minimum. Vibrational frequencies of the tetrahedral isomer were also reported.^{11,15,16}

The phosphorus analogue, PH_4^- , has been paid much less attention theoretically and experimentally to date. Trinquier *et al.*¹⁷ have used a pseudopotential method to investigate two structures, C_{2v} and C_{4v} , and proposed the possibility that a pseudorotation motion connects the two structures. Ortiz¹⁵ has reported structures, vibrational frequencies, and ionization potentials of tetrahedral and trigonal bipyramidal C_{2v} isomers.

Moc and Morokuma¹⁸ have studied the T_d , D_{4h} , C_{4v} , and C_{2v} isomers of XH_4^- and XF_4^- (where X = P, As, Sb, and Bi) using a pseudopotential method as well as all-electron *ab initio* calculations.

We report here the results of *ab initio* calculations on the NH_4^- and PH_4^- ions. First, the structures and the potential energy surfaces of NH_4^- and PH_4^- are explored. Then, the stabilities of the T_d isomers are examined.

Computational Approach

The energetic calculations were performed using locally modified versions of Gaussian 86¹⁹ and Gaussian 88.²⁰ The methods for calculating the energetics of the NH_4^- and PH_4^- isomers are similar in spirit to the additivity of basis set and correlation effects described by Ignacio and Schlegel.²¹

The structures were optimized using second-order Møller–Plesset perturbation theory (MP2)²² with 6-31++G(d,p)²³ and 6-311++G(d,p)²⁴ basis sets, denoted as MP2/6-31++G(d,p) and MP2/6-311++G(d,p), respectively. Due to the diffuse nature of the orbitals in anions, all basis sets are augmented with diffuse p functions for both nitrogen and phosphorus and diffuse s functions for hydrogen to provide more flexibility.²⁵ The matrices of the energy second derivatives (Hessians) were calculated in order to verify the given geometry is a minimum (all eigenvalues of Hessian are positive) or a transition state (the Hessian has one and only one negative eigenvalue). The energy was further refined by fourth-order Møller–Plesset perturbation theory (MP4) with 6-311++G(2d,2p) and 6-311++G(2df,2pd), denoted as MP4/6-311++G(2d,2p) and MP4/6-311++G(2df,2pd). Also, quadratic configuration interaction (QCI) single, double, and perturbative triple (SD(T))²⁶ calculations were performed with the 6-311++G(2d,2p) basis set (QCI/6-311++G(2d,2p)).

The next step is to calculate the contributions of successive improvements in one- and many-electron basis sets to obtain the QCI/6-311++G(2df,2pd) energies by the following additivity scheme:²¹ First, we define four levels of theory

$$A = \text{MP4/6-311++G(2d,2p)}$$

$$B = \text{MP4/6-311++G(2df,2pd)}$$

$$C = \text{QCI/6-311++G(2d,2p)}$$

$$D = \text{QCI/6-311++G(2df,2pd)}$$

At the MP4 level, the improvement due to basis set is

[⊗] Abstract published in *Advance ACS Abstracts*, August 1, 1995.

$$\Delta E(B) = E(B) - E(A)$$

and with the 6-311++G(2d,2p) basis set, the MP4-to-QCI improvement is

$$\Delta E(C) = E(C) - E(A)$$

Assuming additivity of these two improvements, we can estimate $E(D)$ as

$$E(D) = E(A) + \Delta E(B) + \Delta E(C)$$

The MP2/6-31++G(d,p) intrinsic reaction coordinates (IRC: minimum energy paths connecting reactants with products through transition states) are calculated with either the fourth-order Runge-Kutta method²⁷ or the second-order method of Gonzalez and Schlegel²⁸ to check the connectivity of two minima on the PES.

Classical trajectory calculations were performed using the *ab initio* force method,²⁹ sometimes called a dynamic reaction coordinate (DRC) calculation, recently implemented in the GAMESS quantum chemistry package.³⁰ The RHF/6-31++G(d,p) level of theory was used to calculate the trajectories. At the starting point, the equilibrium tetrahedral geometry, an initial kinetic energy of ≤ 35 kcal/mol was given to one of the hydrogens chosen to be on the C_3 axis. The symmetry was turned off during the trajectory calculations, except for the generation of initial tetrahedral geometry, to ensure that there is no artificial constraint in all degrees of freedom.

Nuclear motions obtained from the DRC runs were analyzed by a method developed by Taketsugu and Hirano³¹ in which the appropriately mass-weighted projection of the DRCs onto each normal mode of tetrahedral NH_4^- and PH_4^- was calculated. In other words, the mass-weighted dot product between the displacement of atoms from the equilibrium structure and a particular normal mode was calculated. Only the totally symmetric normal modes possess non-zero projections.

Localized orbitals described by Boys³² were constructed from several geometries obtained by a trajectory calculation to elucidate the nature of bonding during the dissociation of the tetrahedral isomer of PH_4^- into PH_3 and H^- .

Results and Discussions

Structures. Figure 1 shows the MP2-optimized geometries of NH_4^- and PH_4^- . As can be seen from the figure, there are some structurally similar isomers on the PES of NH_4^- and PH_4^- ; both possess C_{2v} (**1b** and **2b**), T_d (**1d** and **2d**), and C_s (**1c** and **2c**) structures.

Structures **1a** and **2a** are rather different. **1a** is the complex, noted earlier, between a hydride ion and ammonia, whereas **2a** can be characterized as a hydrogen molecule complexed with a PH_2^- . The differences in **1a** and **2a** are reflected by the thermodynamic stabilities of the two dissociation asymptotes, *i.e.*, $NH_3 + H^-$ and $NH_2^- + H_2$ vs $PH_3 + H^-$ and $PH_2^- + H_2$. There has been some speculation that **1a** might be the global minimum on the NH_4^- PES.¹⁵ Indeed, **1a** is the lowest minimum found in this study, and **2a** is found to be the lowest energy isomer on the PH_4^- surface.

The bifurcated structure **1c** is a transition state leading in both directions to **1a**. On the other hand, **2c** is a transition state at the MP2/6-31++G(d,p) level of theory, but at the MP2/6-311++G(d,p) level, it is a minimum.

Structure **1e** is unique to NH_4^- ; it is a transition state leading in one direction to the **1a** structure and in the other to **1b**. The latter is also a transition state that leads to **1a**. Structure **2b** is a transition state; however, it is very close to the dissociation limit, $PH_2^- + H_2$.

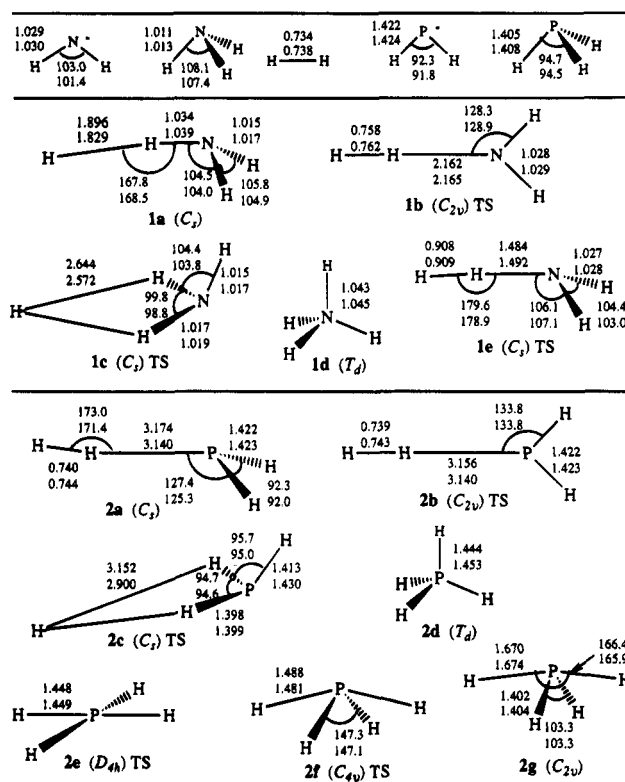
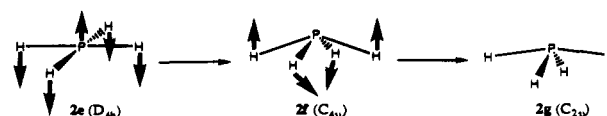


Figure 1. MP2 optimized structures of NH_4^- and PH_4^- and related molecules. The geometries are optimized with the MP2/6-31++G(d,p) (the values at the top) and MP2/6-311++G(d,p) (the values on the bottom) levels of theory. TS indicates that the isomer is a transition state.

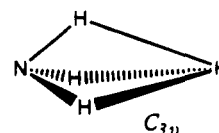
Structures **2e**, **2f**, and **2g** are related through the inversion motion of four hydrogens in the molecule, and they are unique to PH_4^- . The following scheme shows the normal modes associated with **2e** and **2f**.



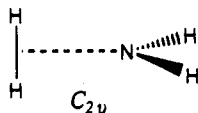
This scheme shows that the motions of the atoms in this process are related to Berry pseudorotation³³ in agreement with the suggestion of Trinquier *et al.*¹⁷ First, the hydrogens in **2e** move in a downward direction (A_{2u} representation) to attain the C_{4v} transition state **2f**. The motions of the hydrogens in the imaginary mode in **2f** have B_1 symmetry such that exchange of the "axial" and "equatorial" hydrogens occurs, leading to the minimum **2g**.

The isomer with D_{4h} symmetry in NH_4^- possesses three imaginary frequencies (one is B_{1g} and other two are E_u), at the MP2/6-31++G(d,p) level of theory. However, at the MP2/6-311++G(d,p) level, it becomes a transition state with one B_{1g} imaginary normal mode.

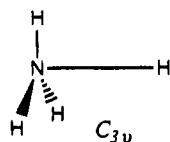
Other structures have been found for NH_4^- ; however, such species are second- or higher-order saddle points. The trifurcated structure shown below is a doubly degenerate second-order saddle point. Moving the attacking hydrogen in the direction of the normal mode vector and reoptimizing the structure leads to structure **1a**.



The complex between NH_2^- and H_2 in C_{2v} symmetry, see below, has a repulsive potential energy. Therefore, the distance between the nitrogen atom and the hydrogen molecule continues to elongate during geometry optimization.



The C_{3v} structure shown below leads to the T_d isomer when optimized.



Cremer and Kraka¹⁰ have calculated the geometries of NH_4^- ions with the MP2/6-31++G(d,p) level. Their results are essentially identical with the corresponding level of the present work, except for **1a** and **1c**, in which their bond lengths between hydride ion and a hydrogen on ammonia in **1a** and between hydride ion and two hydrogens on ammonia in **1c** are off by 0.05 Å. Ortiz¹³ has calculated the geometry of **1a** with the MP2/6-311++G(d,p) level, and his bond lengths are within 0.024 Å of our results; however, the bond length between hydride ion and ammonia is off by 0.15 Å. For **1d**, Cremer and Kraka¹⁰ and Ortiz¹⁵ gave similar results as we have obtained here. Simons and Gutowski¹⁶ have used CASSCF³⁵ and obtained similar results for **1d**.

In the case of PH_4^- , Ortiz¹⁵ has calculated the geometries of **2d** and **2g**, in which the latter species agrees well with the present work. The bond length of **2d** is off by 0.07 Å. Trinquier *et al.*¹⁷ have calculated the geometries of **2g** by limited configuration interaction using pseudopotential with DZP basis sets. Their results agree with our results except for the axial bond length; it is longer by 0.04 Å. Moc and Morokuma¹⁸ have calculated **2d**, **2g**, and **2f** by MP2 using effective core potentials with DZP basis augmented with diffuse functions, and their values are essentially identical with the present study.

Energetics. The total energies of the reference atoms and molecules in this study are shown in Table 1. Table 2 shows the enthalpy differences for NH_4^- with respect to $\text{NH}_3 + \text{H}^-$, and Table 3 shows the analogous enthalpy differences for PH_4^- . As can be seen from the tables, electron correlation is very important in calculating the energetics. The RHF level of theory in the tables is irrelevant in terms of determining energetics, since the geometries are optimized at the MP2 level of theory; the RHF values in the tables are shown as reference. The essential trends are given correctly by MP2. Higher-order perturbation theory, such as MP4 or QCI, is necessary only to determine the quantitative energy differences. The differences in the predicted energetics between the MP4/6-311++G(2d,-2p) and QCI/6-311++G(2d,2p) levels of theory are quite small.

One-electron bases are well converged at 6-311++G(2df,-2pd). The energetics obtained by MP4 with the 6-311++G(2df,2pd) and 6-311++G(2d,2p) basis sets agree to less than 1 kcal/mol, except for **2e** and **2f**. The latter differ by more than 2 kcal/mol. These differences reappear when the QCI/6-311++G(2df,2pd) energies are deduced by the additivity scheme discussed in the previous section. The QCI/6-311++G(2df,2pd) values, except for the two mentioned above, are very similar to the values obtained using the QCI/6-311++G(2d,-2p) level of theory.

TABLE 1: Total Energies and Zero Point Energies of the Reference Atom and Molecules (Energies in Hartrees)

theory	6-31++ G(d,p) ^a	6-311++ G(d,p) ^b	6-311++ G(2d,2p) ^b	6-311++ G(2df,2pd) ^b
NH₃				
RHF	-56.200 85	-56.214 36	-56.217 68	-56.218 74
MP2	-56.396 33	-56.434 68	-56.454 40	-56.475 82
MP4	-56.414 20	-56.454 25	-56.474 42	-56.496 78
QCI			-56.452 89	
ZPE ^c	0.035 34	0.034 89		
NH₂⁻				
RHF	-55.527 42	-55.541 22	-55.544 48	-55.836 14
MP2	-55.735 52	-55.774 58	-55.797 80	-55.818 19
MP4	-55.750 51	-55.791 32	-55.814 95	-55.836 14
QCI			-55.792 13	
ZPE ^c	0.018 99	0.018 86		
PH₃				
RHF	-342.455 03	-342.478 96	-342.482 51	-342.484 75
MP2	-342.592 89	-342.660 45	-342.686 86	-342.711 55
MP4	-342.620 08	-342.690 42	-342.719 10	-342.745 30
QCI			-342.663 92	
ZPE ^c	0.025 23	0.024 98		
PH₂⁻				
RHF	-341.857 79	-341.881 05	-341.883 28	-341.885 10
MP2	-341.992 99	-342.058 91	-342.091 64	-342.114 89
MP4	-342.017 18	-342.085 28	-342.120 36	-342.145 83
QCI			-342.064 84	
ZPE ^c	0.013 58	0.013 45		
H₂				
RHF	-1.131 40	-1.132 50	-1.133 01	-1.133 01
MP2	-1.157 77	-1.160 30	-1.162 80	-1.164 66
MP4	-1.164 69	-1.167 76	-1.170 26	-1.171 74
QCI			-1.170 85	
ZPE ^c	0.010 47	0.010 33		
H⁻				
RHF	-0.487 07	-0.486 93	-0.486 96	-0.486 96
MP2	-0.503 63	-0.505 61	-0.509 58	-0.510 49
MP4	-0.510 39	-0.512 85	-0.518 20	-0.518 59
QCI			-0.519 73	

^a Geometries optimized at MP2/6-31++G(d,p). ^b Geometries optimized at MP2/6-311++G(d,p). ^c ZPE, zero-point energies are calculated at the MP2 level of theory for corresponding basis set.

The G1 theory of Pople *et al.*³⁴ has successfully predicted the heats of formation for many small molecules. Their expected deviation from the experimental heats of formation is about 2 kcal/mol. The energetics calculated in the present work do not include the empirical parameter ("high level correction"); however, the number of bound paired valence electrons are the same for most cases and one larger than the reference $\text{XH}_3 + \text{H}^-$ or $\text{XH}_2^- + \text{H}_2$. So, the expected deviation from experiment is ≤ 4 kcal/mol.

A few attempts have been made to form an ion complex of PH_4^- in a flowing afterglow apparatus; however, they have been unsuccessful thus far.³⁵ The difficulty, as shown in Table 3, is due to the fact that, unlike the NH_4^- PES, the lowest energy complex **2a** is only 1 kcal/mol below the $\text{PH}_2^- + \text{H}_2$ asymptote, and thus, this complex is not very stable. The PES in this region is quite flat, and the structures **2a** and **2b** have essentially the same energy.

The relative energies for $\text{NH}_3 + \text{H}^-$ vs $\text{NH}_2^- + \text{H}_2$ were previously⁸ calculated to be 13 kcal/mol at the HF level, in good agreement with the result obtained here at a similar level of theory. Cremer and Kraka¹⁰ have calculated **1a** to be ≈ 9 kcal/mol more stable relative to $\text{NH}_3 + \text{H}^-$ at the MP2/6-31++G(d,p) level of theory, in agreement with our most accurate calculation. However, their relative energy for tetrahedral NH_4^-

TABLE 2: Enthalpy Difference of NH₄⁻ with Respect to NH₃ + H⁻ (kcal/mol) and Zero-Point Energies (hartree)

theory	6-31++ G(d,p) ^a	6-311++ G(d,p) ^b	6-311++ G(2d,2p) ^b	6-311++ G(2df,2pd) ^b
1a (C_s)				
RHF	-4.4	-4.1	-3.9	-3.9
MP2	-7.8	-8.5	-8.8	-9.0
MP4	-7.5	-8.4	-8.7	-9.0
QCI ^c			-8.5	-8.8
ZPE ^d	0.037 36	0.036 81		
1b (C_{2v}[ts])				
RHF	13.2	12.3	12.6	12.6
MP2	2.5	-2.6	-3.7	-3.8
MP4	0.1	-1.0	-1.3	-1.4
QCI ^c			0.1	0.1
ZPE ^d	0.033 35	0.032 87		
1c (C_s)				
RHF	-4.3	-4.1	-3.9	-3.8
MP2	-2.0	-6.7	-6.7	-6.9
MP4	-6.1	-6.6	-6.9	-7.0
QCI ^c			-7.0	-7.1
ZPE ^d	0.036 50	0.036 06		
1d (T_d)				
RHF	16.7	17.0	17.5	17.4
MP2	11.5	8.3	11.9	11.8
MP4	6.0	7.5	12.1	11.5
QCI ^c			12.7	12.2
ZPE ^d	0.044 89	0.044 28		
1e (C_s[ts])				
RHF	17.0	16.5	16.8	16.8
MP2	4.6	-1.2	-2.0	-2.5
MP4	2.4	0.3	0.1	-0.4
QCI ^c			1.5	1.0
ZPE ^d	0.037 36	0.032 03		
NH₂⁻ + H₂				
RHF	14.6	13.8	13.5	13.5
MP2	0.5	-0.2	-1.5	-1.4
MP4	2.2	1.4	1.1	1.1
QCI ^c			2.5	2.5

^a Geometries are optimized at MP2/6-31++G(d,p). ^b Geometries are optimized at MP2/6-311++G(d,p). ^c QCI/6-311++G(2d,2p) results are of actual calculations and QCI/6-311++G(2df,2pd) values are deduced by assuming additivity (see text). ^d ZPE, zero-point energies are calculated at the MP2 level of theory for corresponding basis set.

(1d) is 1.3 kcal/mol. This is underestimated by over 10 kcal/mol in comparison to the present work. Cardy *et al.*¹¹ have calculated the relative energies of 1a and 1d using the CISDQ/4-31++G(d,p) level of theory and have obtained -6.3 and 6.1 kcal/mol relative to NH₃ + H⁻, respectively. The relative energy of 1d is underestimated by ≈6 kcal/mol in comparison to the present work.

Trinquier *et al.*¹⁷ have calculated the relative energy of 2g with respect to PH₃ + H⁻ using HF/DZP+ and CI/DZP+ to be 4.8 and 1.4 kcal/mol, respectively. Their CI result (1.4 kcal/mol) is underestimated by 6 kcal/mol using the QCI/6-311++G(2df,2pd) levels of the present work. They have also reported that the structure 2f is higher in energy than 2g by 9 kcal/mol at the HF level of theory. The result of the present work estimates the energy difference between 2f and 2g to be ≈5 kcal/mol. More recently, the relative energies calculated for 2e, 2f, and 2g by Moc and Morokuma¹⁸ are in good agreement with our best, QCI/6-311++G(2df,2pd), results.

Stability of Tetrahedral Isomers. The tetrahedral isomers of NH₄⁻ and PH₄⁻ are not connected to any other isomers through the IRCs studied here. It is important to understand the origin of the stability and the nature of bonding of these tetrahedral isomers. Two tools that are useful for this endeavor are the dynamic reaction coordinate (DRC) analysis and the ionization potentials.

TABLE 3: Enthalpy Difference of PH₄⁻ with Respect to PH₃ + H⁻ (kcal/mol) and Zero-Point Energies (hartree)

theory	6-31++ G(d,p) ^a	6-311++ G(d,p) ^b	6-311++ G(2d,2p) ^b	6-311++ G(2df,2pd) ^b
2a (C_s)				
RHF	-29.2	-29.4	-28.9	-28.6
MP2	-34.6	-34.0	-37.0	-36.7
MP4	-32.8	-32.0	-34.1	-34.4
QCI ^c			-33.0	-33.5
ZPE ^d	0.026 89	0.026 79		
2b (C_{2v}[ts])				
RHF	-29.6	-30.0	-29.5	-29.2
MP2	-34.8	-34.2	-37.2	-37.0
MP4	-33.0	-32.2	-34.4	-34.7
QCI ^c			-33.2	-33.8
ZPE ^d	0.026 44	0.026 12		
2c (C_s)				
RHF	-2.0	-1.4	-1.8	-1.9
MP2	-2.8	-3.1	-4.1	-4.2
MP4	-2.6	-3.0	-4.1	-4.2
QCI ^c			-4.3	-4.1
ZPE ^d	0.025 74	0.026 05		
2d (T_d)				
RHF	43.6	42.2	42.0	41.4
MP2	32.8	31.7	35.9	35.9
MP4	32.6	31.4	36.8	36.4
QCI ^c			37.4	37.0
ZPE ^d	0.025 55	0.023 84		
2e (D_{4h})				
RHF	22.8	22.1	21.3	20.7
MP2	10.5	8.3	5.0	1.8
MP4	12.0	9.7	7.5	4.3
QCI ^c			8.8	5.3
ZPE ^d	0.030 73	0.030 49		
2f (C_{4v})				
RHF	14.0	13.2	12.5	11.5
MP2	4.0	1.4	-1.0	-3.3
MP4	5.4	2.4	0.6	-1.6
QCI ^c			1.8	-0.6
ZPE ^d	0.029 30	0.028 98		
2g (C_{2v})				
RHF	6.7	6.2	5.1	3.4
MP2	-0.9	-3.4	-6.7	-8.2
MP4	0.4	-2.6	-5.6	-6.9
QCI ^c			-4.4	-5.2
ZPE ^d	0.027 99	0.027 78		
PH₂⁻ + H₂				
RHF	-31.0	-30.6	-30.1	-28.6
MP2	-36.4	-34.1	-37.2	-36.8
MP4	-34.6	-32.0	-34.2	-34.4
QCI ^c			-32.4	-32.3

^a Geometries are optimized at MP2/6-31++G(d,p). ^b Geometries are optimized at MP2/6-311++G(d,p). ^c QCI/6-311++G(2d,2p) results are of actual calculations, and QCI/6-311++G(2df,2pd) values are deduced by assuming additivity (see text). ^d ZPE, zero-point energies are calculated at the MP2 level of theory for corresponding basis set.

Cardy *et al.*¹¹ have investigated the reaction profile of tetrahedral NH₄⁻, in which one of the hydrogens is pulled outward in the direction along the C_{3v} dissociation pathway, by fixing the dissociating bond distance at successively larger values and optimizing the remaining geometric parameters. Their CISDQ/DZ+P barrier to dissociation along the C_{3v} path is 18.6 kcal/mol relative to the tetrahedral structure.

It is indeed possible that there is no transition state associated with the T_d structures due to their high symmetry. On the H-C≡P potential energy surface, for example, there is no transition state.³⁶ Instead, there is a second-order saddle point, possessing doubly degenerate imaginary vibration modes, to convert H-C≡P to C=P-H. This is indicative of having high (C_{∞v}) symmetry. The tetrahedral structures of NH₄⁻ and PH₄⁻ might fall into such a category, and there may not be a transition

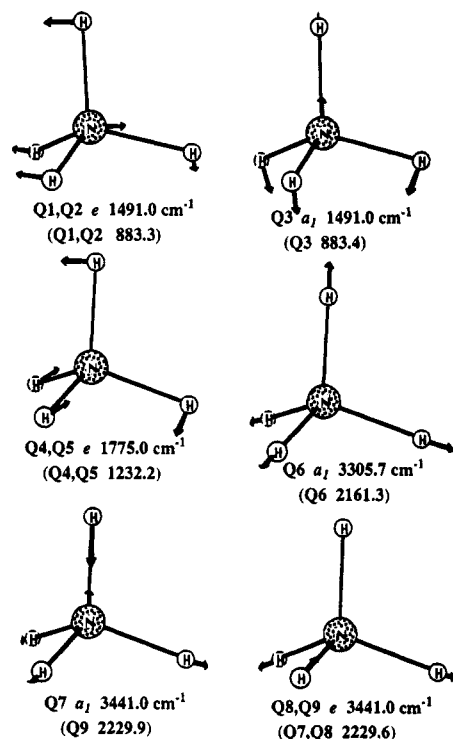


Figure 2. Normal modes of tetrahedral NH_4^- and PH_4^- . Normal mode vectors and their frequencies are shown in terms of C_{3v} symmetry. The values in parentheses are for PH_4^- .

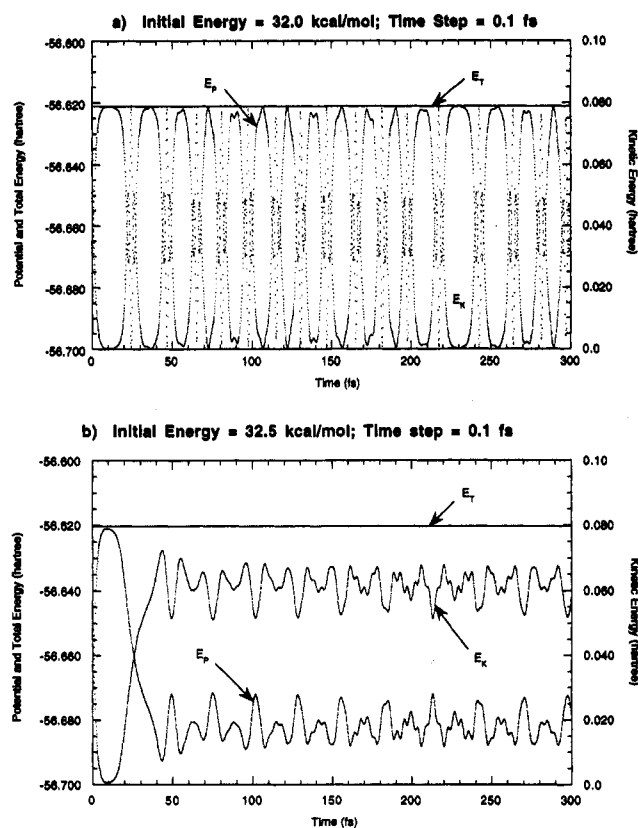


Figure 3. Energy change during trajectory calculations of NH_4^- . Total energy (E_T), potential energy (E_P), and kinetic energy (E_K) are plotted with respect to time (in femtosecond). (a) Initial kinetic energy (32.0 kcal/mol) is given to a hydrogen atom in the C_3 axis direction. (b) Initial kinetic energy is 32.5 kcal/mol.

state that connects the T_d structures to other isomers. To investigate this possibility in a qualitative manner, we turn to a dynamic reaction coordinate analysis.

(a) DRC Analysis. A trajectory calculation initiated by

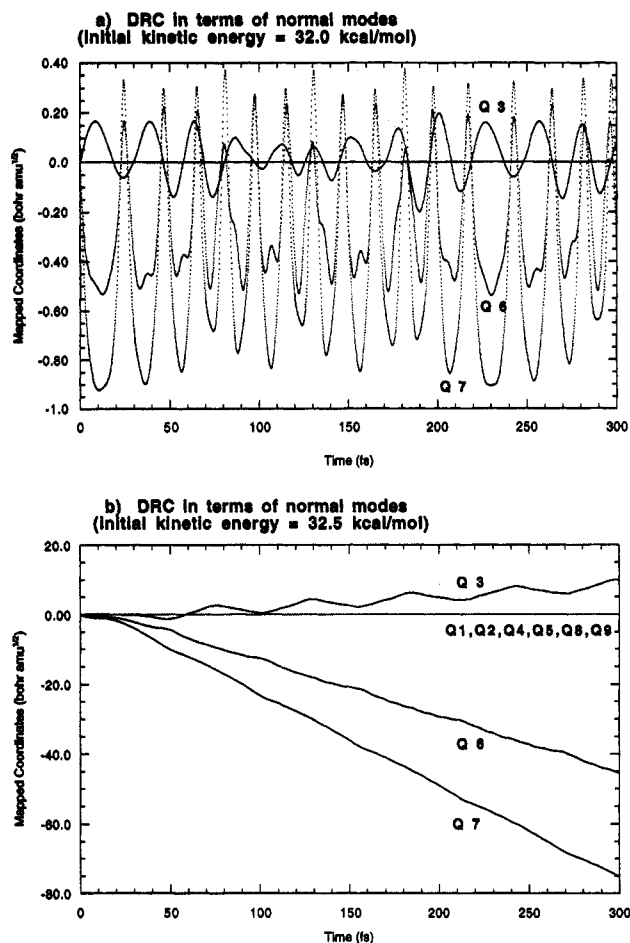


Figure 4. DRC of NH_4^- in terms of normal modes of vibration. The trajectory coordinates are mapped in terms of normal modes of tetrahedral NH_4^- in C_{3v} symmetry. (a) The normal mode contributions to the trajectory calculated with an initial kinetic energy of 32.0 kcal/mol given to a hydrogen atom on the C_3 axis. (b) 32.5 kcal/mol.

giving an initial kinetic energy to a hydrogen in a C_s plane was carried out. However, this resulted only in molecular rotation; therefore, no further C_s trajectory was calculated. Other trajectories (using scissoring motions, Q4 and Q5 in Figure 2) were considered; however, this C_{2v} process must occur at very high energy, since two bond breakings must occur in order to have a reaction in the C_{2v} path, to preserve symmetry. Therefore, such a reaction is less likely to occur, and therefore, no trajectory was calculated.

Trajectories with C_{3v} symmetry were calculated for up to 300 fs with an initial kinetic energy ≤ 35 kcal/mol. No dissociation was observed until 32.5 kcal/mol of kinetic energy was introduced. Figure 2 shows the normal modes of tetrahedral NH_4^- in C_{3v} symmetry. Since a DRC preserves the symmetry of the reaction coordinate,³¹ one expects those normal mode vibrations that are symmetric with respect to C_{3v} symmetry (A_1 modes Q3, Q6, and Q7 of Figure 4) to be the ones that participate in the bond-breaking process to obtain ammonia and a hydride ion.

The energy changes during the trajectory calculations (initial kinetic energy = 32.0 and 32.5 kcal/mol), giving energy to one of the hydrogens chosen as the C_{3v} axis in NH_4^- , are shown in Figure 3. The total energy is, of course, conserved in these calculations, and kinetic and potential energies oscillate in opposite directions. The molecule undergoes large amplitude motions during the trajectory with an initial kinetic energy of 32.0 kcal/mol, which is the threshold of the bond-breaking process at the RHF/6-31++G(d,p) level of theory. The nuclear

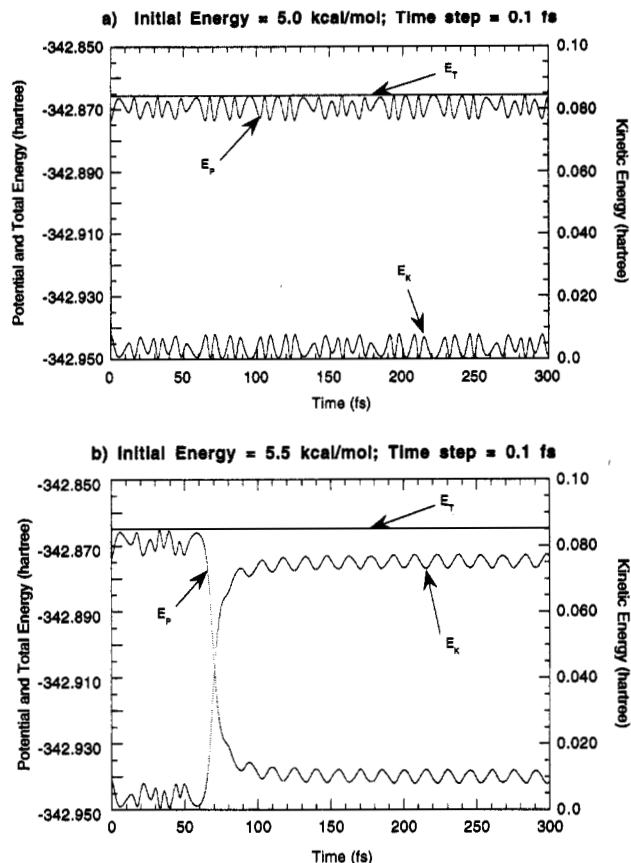


Figure 5. Energy change during trajectory calculations of PH_4^- . Total energy (E_T), potential energy (E_P), and kinetic energy (E_K) are plotted with respect to time (in femtosecond). (a) Initial kinetic energy (5.0 kcal/mol) is given to a hydrogen atom in the C_3 axis direction. (b) Initial kinetic energy is 5.5 kcal/mol.

motions can be described by mapping the DRC onto the normal modes of vibration.³¹ Figure 4 shows the plots of these projected coordinates. As expected, the only normal modes that can contribute in the C_{3v} dissociation path are Q3, Q6, and Q7. Q6 and Q7 are in resonance with each other, while Q3 contributes in the opposite direction during the large amplitude motions shown in Figure 4a. The axis bond compresses and stretches from 0.83 to 1.60 Å, corresponding to about 80–156% of the equilibrium bond length.

Dissociation would occur for an initial kinetic energy of 32.5 kcal/mol given to the axial hydrogen. Since this energy is rather high, the dissociation occurs during the first energy oscillation. The amplitudes of oscillation after dissociation takes place correspond roughly to the inversion barrier of ammonia, and the kinetic energy of the dissociated hydride ion is about 0.06 hartree (1.6 eV), as shown in Figure 3b.

The threshold of dissociation in PH_4^- is only 5.0 kcal/mol, quite different from NH_4^- . The nuclear motion is still oscillatory at 5.0 kcal/mol, but it is much smaller than that of NH_4^- . Figure 5 shows the energy change during the trajectory calculations for PH_4^- . Dissociation (Figure 5) does not take place until the seventh energy oscillation. The energetic profiles are similar to those found for NH_4^- except for the smaller amplitudes. Figure 6 shows the plots of the vibrational mapping of the DRC. The oscillations of the mapped coordinates are rather different from the NH_4^- . In both cases, above and below the threshold, the oscillatory period of Q3 is about twice as large as those for Q6 and Q9. In fact, the dissociation occurs after completing one period of Q3 vibrational motion. Below the threshold, the axial bond compresses and stretches from about 1.23 to 1.665 Å, which is about 90–112% of the

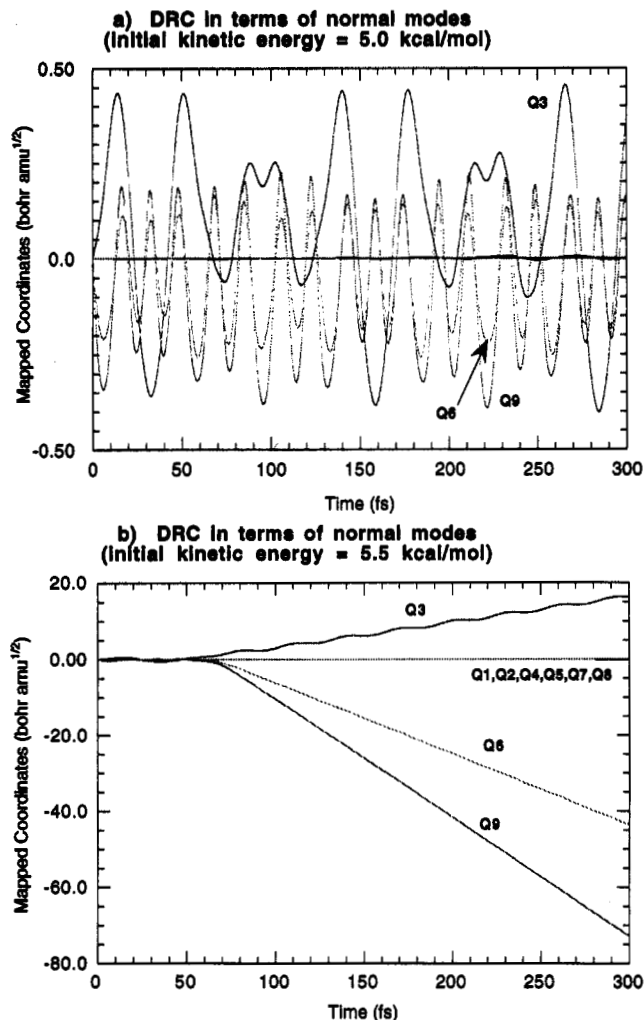


Figure 6. DRC of PH_4^- in terms of normal modes of vibration. The trajectory coordinates are mapped in terms of normal modes of tetrahedral PH_4^- in C_{3v} symmetry. (a) The normal mode contributions to the trajectory calculated with an initial kinetic energy of 5.0 kcal/mol given to a hydrogen atom on the C_3 axis. (b) 5.5 kcal/mol.

equilibrium bond length. This is due to the fact that only a small amount of energy is given to the bond of interest. As a consequence, the phosphine has a small amount of vibrational energy. The dissociated hydride ion in PH_4^- has a larger kinetic energy (0.075 hartree or 2.0 eV) than that of NH_4^- , despite the smaller amount of initial energy. Referring to Table 3, note that the sum of the initial kinetic energy plus the energy released by breaking the $\text{XH}_3\text{-H}^-$ bond ($T_d \rightarrow \text{XH}_3 + \text{H}^-$) is about the same for $\text{X} = \text{N}, \text{P}$. It is sensible therefore that the H^- receding from the heavier PH_3 will have greater kinetic energy.

Figure 7 shows the localized orbitals of PH_4^- constructed at several geometries during a trajectory calculation to show how orbitals are rearranged during dissociation. The left-hand side of Figure 7a is a σ -bonding orbital, and as the time progresses in the dissociation process, the orbital becomes the s^2 orbital of H^- . On the other hand, the diffuse s-type orbital, double-Rydberg orbital,³⁷ on the right-hand side of Figure 7 becomes a lone pair of PH_3 as time progresses. Figure 7b, taken at the highest energy geometry, is at the threshold of bond dissociation which occurs at 58.5 fs. As the bond stretches further, the orbital becomes more diffuse in nature.

(b) Ionization Potentials. There is only one experimental ionization potential dealing with the tetrahedral isomer of NH_4^- in the literature.^{7b} The first ionization potential for NH_4^- is 0.472 eV, obtained by photoelectron spectroscopy, and the

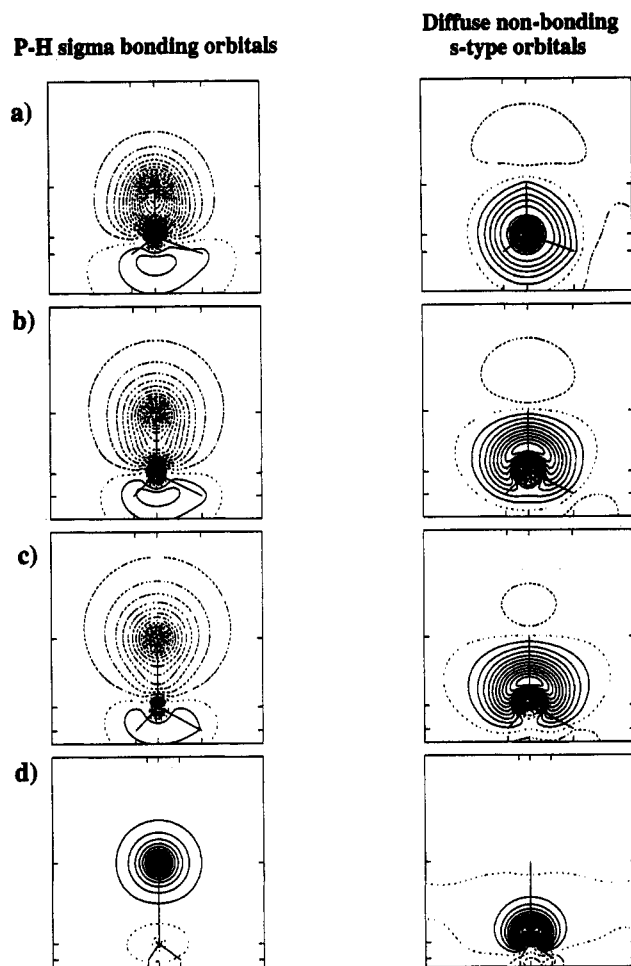


Figure 7. Localized orbitals of PH_4^- for the geometries taken during the trajectory run. Each contour is drawn at $0.02 \text{ bohr}^{-3/2}$. The geometries at which the localized orbitals are constructed are (a) at equilibrium tetrahedral structure (bond length = 1.419 Å), (b) at 58.5 fs, the highest energy point (1.720 Å), (c) at 65.0 fs (1.960 Å), and (d) at 80.0 fs (4.206 Å).

structure of this isomer is suspected to be tetrahedral. The ionization potential has the same value as the electron affinity of neutral NH_4 , indicating that the structure of NH_4^- is similar to the neutral.

First and second vertical ionization potentials (Table 4) of the tetrahedral isomers were calculated with several levels of theory by taking differences between the energies calculated at the respective levels of theory between anion and neutral for the first IP and between neutral and cation for the second IP. The first ionization potential of NH_4^- is -0.6 and -0.04 eV at the Hartree-Fock and MP2 levels of theory, respectively, using the 6-31++G(d,p) basis set. This means that the electron in the highest occupied orbital is unstable and would therefore autoionize. A full valence CASSCF³⁸ calculation does not correct the sign of the ionization potential. Dynamical electron correlation is very important, based on the RHF-MP2 difference, and at least MP4 is needed to obtain the correct sign. Furthermore, the effect of basis set is also crucial for calculating the IP of the anion. Inclusion of two diffuse functions at each center is needed to obtain an IP close to the experimental value. A similar conclusion was indicated earlier by Ortiz.¹³ The IP obtained with the QCI/6-311(2+,2+)G(2df,2pd) (not by additivity, but with the frozen core approximation) is essentially the same as the one obtained with the UMP4/6-31(2+,2+)G(d,p) level of theory. The second ionization potential is large and positive, indicating that the neutral radical species is stable toward autoionization.

TABLE 4: Calculated Vertical Ionization Potentials (IP) of the Tetrahedral Isomers of NH_4^- and PH_4^- (in eV)^a

	first IP	second IP
NH_4^-		
UHF/6-31++G(d,p)	-0.58	4.06
(10,8)CASSCF/6-31++G(d,p)	-0.61	3.11
UMP2/6-31++G(d,p)	-0.05	4.42
UMP4/6-31++G(d,p)	0.12	4.44
QCISD(T)/6-31++G(d,p)	0.12	4.44
UHF/6-311++G(d,p)	-0.18	4.07
UMP2/6-311++G(d,p)	-0.22	4.42
UMP4/6-311++G(d,p)	0.39	4.44
UHF/6-311++G(d,p)	-0.58	4.06
QCISD(T)/6-311++G(2df,2pd)	0.16	4.53
UHF/6-311(2+,2+)G(d,p)	-0.18	4.07
UMP2/6-311(2+,2+)G(d,p)	0.24	4.45
UMP4/6-311(2+,2+)G(d,p)	0.40	4.47
QCISD(T)/6-311(2+,2+)G(d,p)	0.40	4.48
QCISD(T)/6-311(2+,2+)G(2df,2pd)	0.39	4.53
experiment ^b	0.472	
PH_4^-		
UHF/6-31++G(d,p)	-0.64	3.58
QCISD(T)/6-31++G(d,p)	0.01	4.05
UHF/6-311++G(d,p)	-0.64	3.58
UMP2/6-311++G(d,p)	-0.08	4.05
UMP4/6-311++G(d,p)	0.04	4.10
QCISD(T)/6-311++G(2df,2pd)	0.06	4.18
QCISD(T)/6-311(2+,2+)G(d,p)	0.30	4.12
QCISD(T)/6-311(2+,2+)G(2df,2pd)	0.33	4.19

^a Ionization potentials are calculated from the geometries of the anion optimized at the MP2 level of theory with either 6-31++G(d,p) or 6-311++G(d,p). The frozen core approximation is used to obtain the QCI values; others are done with the inclusion of core excitations. 6-31(2+,2+)G indicates that two diffuse functions are used at each center with the 6-31G basis. ^b See ref 7b.

A similar trend occurs for PH_4^- . As the level of theory is improved, the first ionization potential goes from negative to slightly positive. The second ionization potential is large and positive, indicating that the neutral radical is stable toward autoionization. The first IP for tetrahedral PH_4^- is slightly less than that obtained for NH_4^- . By starting from NH_4^+ and PH_4^+ , the electron attachment process to make the neutral radical species should not be difficult. By using these neutral radicals, trying to attach an electron is perhaps more difficult. Because of the apparently small dissociation barrier calculated by the DRC, even though the first IP is similar to the NH_4^- , observation of the tetrahedral isomer of PH_4^- is expected to be more difficult.

Conclusions

We have examined the PES of NH_4^- and PH_4^- , and the energy differences are deduced by additivity rules to obtain the QCI/6-311++G(2df,2pd) energies. The most stable structure is a complex between an ammonia molecule and a hydride ion and a complex between H_2 and PH_2^- . The highest energy isomers in both cases are tetrahedral structures.

DRC calculations show that these tetrahedral structures could dissociate into a hydride ion and XH_3 . In the case of NH_4^- , it was shown that the energy needed to break an N-H bond in C_{3v} dissociation path is 32.5 kcal/mol. For PH_4^- , the dissociation occurs when 5.5 kcal/mol is given to the P-H bond. These values are likely to be reduced by several kcal/mol upon the introduction of electron correlation and improvement of the basis set.

The first ionization potential predicted for tetrahedral NH_4^- is close to the experimental value, and therefore, this anion is

stable. Similarly, the first IP for the tetrahedral PH_4^- is somewhat smaller than that for NH_4^- but is predicted to be positive (0.32 eV). The neutral radicals, on the other hand, are stable; both second IP's are about 4 eV.

Since the dissociation of the tetrahedral NH_4^- ion appears to require considerably more energy than ionization to the neutral, it is likely that the molecule will autoionize before it has a chance to dissociate. This is less likely to be the case for tetrahedral PH_4^- .

Acknowledgment. This work was supported in part by a grant from the Air Force Office of Scientific Research (F49620-95-1-0077). The calculations were performed in part on the North Dakota State University IBM ES9000 computer under a joint study agreement with IBM and in part on an IBM RS6000/530 obtained via a grant to M.S.G. from AFOSR. Some calculations were performed on IBM RS6000/350 computers made available by the Iowa State University. We acknowledge helpful discussions with Dr. Tetsuya Taketsugu on normal mode mapping analysis.

References and Notes

- (1) (a) Tandura, S. N.; Voronkov, M. G.; Alekseev, N. V. *Top. Curr. Chem.* **1986**, *131*, 99. (b) Curriu, R. J. P. *J. Organomet.* **1990**, *400*, 81. (c) Chuit, C.; Corriu, R. J. P.; Reye, C.; Young, J. C. *Chem. Rev.* **1993**, *93*, 1371.
- (2) Windus, T. L.; Gordon, M. S.; Davis, L. P.; Burgraf, L. W. *J. Am. Chem. Soc.* **1990**, *112*, 7167.
- (3) Pauling, L. *The Nature of the Chemical Bond*, 3rd ed.; Cornell University: Ithaca, NY, 1960; p 145.
- (4) Reed, A. E.; Schleyer, P. v. R. *J. Am. Chem. Soc.* **1990**, *112*, 1434.
- (5) Cooper, D. L.; Cunningham, T. P.; Gerratt, J.; Karadakov, P. B.; Rimondi, M. *J. Am. Chem. Soc.* **1994**, *116*, 4414.
- (6) Kleingeld, J. C.; Ingemann, S.; Jalonen, J. E.; Nibbering, N. M. M. *J. Am. Chem. Soc.* **1983**, *105*, 2474.
- (7) (a) Coe, J. V.; Snodgrass, J. T.; Freidhoff, C. B.; McHugh, K. M.; Bowen, K. H. *J. Chem. Phys.* **1985**, *83*, 3169. (b) Snodgrass, J. T.; Coe, J. V.; Freidhoff, C. B.; McHugh, K. M.; Bowen, K. H. *Faraday Discuss. Chem. Soc.* **1988**, *86*, 241.
- (8) Ritchie, C. D.; King, H. *J. Am. Chem. Soc.* **1968**, *90*, 838.
- (9) Kalcher, J.; Rosmus, P.; Quack, M. *Can. J. Phys.* **1984**, *62*, 1323.
- (10) Cremer, D.; Kraka, E. *J. Am. Chem. Soc.* **1986**, *90*, 33.
- (11) Cardy, H.; Larrieu, C.; Dargelos, A. *Chem. Phys. Lett.* **1986**, *131*, 507.
- (12) Hirao, K.; Kawai, E. *THEOCHEM* **1987**, *149*, 391.
- (13) Ortiz, J. V. *J. Chem. Phys.* **1987**, *87*, 3557.
- (14) Gutowski, M.; Simons, J.; Hernandez, R.; Taylor, H. L. *J. Phys. Chem.* **1988**, *92*, 6179.
- (15) Ortiz, J. V. *J. Phys. Chem.* **1990**, *94*, 4762.
- (16) Simons, J.; Gutowski, M. *Chem. Rev.* **1991**, *91*, 669.
- (17) Trinquier, G.; Daudey, J. P.; Caruana, G.; Madaule, Y. *J. Am. Chem. Soc.* **1984**, *106*, 4794.
- (18) Moc, J.; Morokuma, K. *Inorg. Chem.* **1994**, *33*, 551.
- (19) Frisch, M. J.; Binkley, J. S.; Schlegel, H. B.; Raghavachari, K.; Melius, C. F.; Martin, R. L.; Stewart, J. J. P.; Borowicz, F. W.; Rohlfing, C. M.; Kahn, L. R.; DeFree, D. J.; Seeger, R.; Whiteside, R. A.; Fox, D. J.; Fluder, E. M.; Pople, J. A. Carnegie-Mellon Quantum Chem. Publishing Unit, Pittsburgh, PA 15213.
- (20) Frisch, M. J.; Head-Gordon, M.; Schlegel, H. B.; Raghavachari, K.; Binkley, J. S.; Gonzalez, C.; Defrees, D. J.; Fox, D. J.; Whiteside, R. A.; Seeger, R.; Melius, C. F.; Baker, J.; Martin, R. L.; Kahn, L. R.; Stewart, J. J. P.; Fluder, E. M.; Topiol, S.; Pople, J. A. Gaussian 88, Gaussian Inc., Pittsburgh, PA, 1988.
- (21) Ignacio, E. W.; Schlegel, H. B. *J. Comput. Chem.* **1991**, *12*, 751.
- (22) Møller, C.; Plesset, M. S. *Phys. Rev.* **1934**, *46*, 618.
- (23) (a) Hehre, W. J.; Ditchfield, R.; Pople, J. A. *J. Chem. Phys.* **1971**, *54*, 724. (b) Francl, M. M.; Pietro, W. J.; Hehre, W. J.; Binkley, J. S.; Gordon, M. S.; DeFrees, D. J.; Pople, J. A. *J. Chem. Phys.* **1982**, *77*, 3654.
- (24) (a) Raghavachari, K.; Binkley, J. S.; Seeger, R.; Pople, J. A. *J. Chem. Phys.* **1980**, *72*, 650. (b) McLean, A. D.; Chandler, G. S. *J. Chem. Phys.* **1980**, *72*, 5639.
- (25) We have used the following diffuse Gaussian exponents: N, 0.0639; P, 0.0348; H, 0.0360.
- (26) Pople, J. A.; Head-Gordon, M.; Raghavachari, K. *J. Chem. Phys.* **1987**, *87*, 5968.
- (27) Baldrige, K. K.; Gordon, M. S.; Steckler, R.; Truhler, D. G. *J. Phys. Chem.* **1989**, *93*, 5107.
- (28) (a) Gonzales, C.; Schlegel, H. B. *J. Phys. Chem.* **1990**, *94*, 5523. (b) Gonzales, C.; Schlegel, H. B. *J. Chem. Phys.* **1991**, *95*, 5853.
- (29) (a) Stewart, J. J. P.; Davis, L. P.; Burgraff, L. W. *J. Comput. Chem.* **1987**, *8*, 1117. (b) Maluendes, S. A.; Dupuis, M. *J. Chem. Phys.* **1990**, *93*, 5902.
- (30) (a) Schmidt, M. W.; Baldrige, K. K.; Boatz, J. A.; Elbert, S. T.; Gordon, M. S.; Jensen, J. H.; Koseki, S.; Matsunaga, N.; Nguyen, K. A.; Su, S.; Windus, T. L.; Dupuis, M.; Montgomery, J. A. *J. Comput. Chem.* **1993**, *14*, 1347. (b) Contact Mike Schmidt at mike@si.fi.ameslab.gov concerning this program.
- (31) (a) Taketsugu, T.; Hirano, T. *J. Phys. Chem.*, submitted. (b) For application, see: Taketsugu, T.; Gordon, M. S. *J. Phys. Chem.*, submitted.
- (32) Boys, S. F. in *Quantum Science of Atoms, Molecules, and Solids*; Lowdin, P. O., Ed.; Academic: New York, 1966; p 253.
- (33) (a) Berry, R. S. *J. Chem. Phys.* **1960**, *32*, 933. (b) Mislow, K. *Acc. Chem. Res.* **1970**, *3*, 321.
- (34) Pople, J. A.; Head-Gordon, M.; Fox, D. J.; Raghavachari, K.; Curtiss, L. *J. Chem. Phys.* **1989**, *90*, 5622.
- (35) Bierbaum, V. Private communication, 1990.
- (36) Dykema, K. A.; Gordon, M. S. *J. Am. Chem. Soc.* **1985**, *107*, 4535.
- (37) A double-Rydberg ion is described as two electrons in a diffuse Rydberg-type orbital interacting with the cationic core providing an electrostatic potential. See refs 14–16 for explanation.
- (38) CASSCF, Complete Active Space Self-Consistent Field or FORS-MSCF: Ruedenberg, K.; Schmidt, M. W.; Gilbert, M. M.; Elbert, S. T. *Chem. Phys.* **1982**, *71*, 41, 51 and 65.

JP9511010